Journal of Cultural Heritage 62 (2023) 422–429

Contents lists available at ScienceDirect

Journal of Cultural Heritage

journal homepage: www.elsevier.com/locate/culher

Case study

Disclosing the composition of the Renaissance thin uniface metallic strikings by Alessandro Cesati (mid-16th century) from the Bargello Museum using non-invasive analyses

Francesca Di Turo[a,*], Giulia Daniele[b], Paola D'Agostino[c], Lucia Simonato[b], Fabio Beltram[a], Pasqualantonio Pingue[a]

[a] National Enterprise for nanoScience and nanoTechnology (NEST), Scuola Normale Superiore, Piazza dei Cavalieri 7, 56126, Pisa, Italy
[b] Laboratorio di Documentazione Storico-Artistica (DocStAr), Scuola Normale Superiore, Piazza dei Cavalieri 7, 56126, Pisa, Italy
[c] National Museum of Bargello, Via del Proconsolo 4, 50122, Firenze, Italy

ARTICLE INFO

Article history:
Received 11 November 2022
Accepted 30 May 2023
Available online 7 July 2023

Keywords:
Renaissance medals
Surface characterization
Alloy composition
Non-destructive analysis
SEM-EDS

ABSTRACT

This study focuses on a series of thin uniface strikings preserved in the Bargello Museum (Florence, Italy), analysed using non-destructive and non-invasive techniques. These specimens were created in Rome by Italo-Greek sixteenth-century goldsmith and medalist Alessandro Cesati, called 'Grechetto', for Pope Paul III (1534–1549 A.D.) and Pope Julius III (1550–1555 A.D.). The samples were studied to explore the chemical composition and the surface morphology of the alloy since they are characterized by thin metal uniface strikings, representing a truly unique case study.

New information about production technique, alloy composition, and on the use of these foils as prototypes by the artist are gained thanks to the analysis of such exemplars. A scanning electron microscope with an energy dispersive system (SEM-EDS) shows that the pieces are characterized by a surface enriched in Ag (up to 48 wt%) and/or Au (up to 6.3 wt%), whereas the back side shows an Sn-Pb alloy. In this specimen, Sn reaches 59.9 wt%, and Pb is up to 64.3 wt%, displaying a typical microstructure of Pb islands dispersed in an Sn matrix. Moreover, the absence of a preferential orientation of such lead clusters implies that the medal was subjected to very soft mechanical processing, such as hammering. FTIR analysis detected the use of a resin to glue the foils onto a different substrate, suggesting that Cesati also used these strikings to produce medallic prototypes to send to friends and patrons outside Rome.

Introduction

The study of medals benefits from an interdisciplinary approach that provides interesting new data about the artist, the production technology, and the raw materials used. There is little scientific research into medals for several reasons, which include, the higher availability of coin samples compared to medals, the need to study corrosion products of coins found in archeological contexts, and the practical difficulties in analysing medals in museums. However, in spite of these difficulties, in-depth study of medals, which should not be equated with coins, is needed to fill this lacuna.

While ancient coins were produced by an authority with specific metals and weights corresponding to their commercial value, medals, which were invented in the 15th century, were mostly used as political and commemorative objects, and anyone, even private citizens, could commission them. There were no standards for material, weight, or size, and medals with diameters ranging between 2 and 10 cm have been found. Different alloys were used to reproduce the same specimen in series. In fact, depending on the power of the commissioner, medals could also be mass-produced to commemorate a private event, a military victory, or a jubilee, and the importance of the event could, in some cases, also determine the quantities of medals produced [1]. The medals could be duplicated even years after the first production, and today, this is one of the major problems in studying such objects [2]. Medals are round with two sides: the obverse and the reverse. The obverse shows the portrait of the medal's commissioner with the inscription, whereas the reverse usually features text and images displaying details about the portrayed person or the commemorative occasion, usually an allegory or a historical or religious event [3].

In the early modern age, medals were made with two different methods: casting or striking. The casting process being the most

* Corresponding author.
E-mail address: francesca.dituro@sns.it (F. Di Turo).

https://doi.org/10.1016/j.culher.2023.05.034
1296-2074/

common [1,4–6]. In this case, the artist realised an image in wax, adding the details using direct modeling or adding the letters to a mold made of ashes, salt, water, glue binder and other heterogeneous materials. The molten metal could be a bronze or copper alloy, gold or silver, and was poured into the mold and cooled. After removing the cast medal, excess metal and other irregularities were removed. Striking, on the other hand, consisted of forcefully stamping images, numbers, letters, and so on, onto a metal which were impressed in negative onto the observe and reverse through two dies [3,4].

As mentioned above, the scientific literature concerning the analysis of medals is very limited, restricting the possibility of comparing data from various collections. However, these medals can be studied through established methods and approaches in the field of coins [7–11], while not losing sight of the substantial differences between medals and coins. Farrell [12] discuss the possibility of analysing coins and medals using a non-destructive approach, that is the pillar of diagnostic philosophy. Some studies focus on the differences between cast and struck medals: cast medals usually display pits and air bubbles, whereas struck medals have a smoother surface. These characteristics are easily identifiable with an optical microscope [13,14]. The differences between cast, struck, and electroformed medals by means of X-ray diffraction are reported by Wharton, who identifies the later reproduction of the Renaissance medals [15]. Data coming from two-hundred medals from the collection of the National Gallery of Art in Washington are reported in the work of Glinsman and Hayek [16]. The researchers, performing X-ray fluorescence (XRF) analysis, highlight the complexity of the surface composition of the medals, which were mainly made of copper, tin, lead, arsenic, iron, silver, and nickel. This is the largest analytical campaign conducted on medals to date.

Today it is possible to perform analysis with high-performance instrumentations, but the difficulty of moving the samples from the museums and the need to choose only non-destructive analyses are the two main limitations in the field of diagnostics. This problem is amplified in the case of medals, which are usually part of museum collections. We faced these limitations in the present case study, circumventing them through the combined use of *in situ* analysis and non-destructive investigations.

The present research aims to investigate the surface composition, the technology production, and art-historical implications of three significant exemplars preserved in the notable collection of Renaissance and Baroque medals in the Bargello Museum, Florence. The chosen specimens are a truly unique case study since they are thin uniface metal strikings, so they can not be considered 'normal' medals. In one of these cases, the two foils are pasted to a central core in order to simulate the aspect of a real medal. The other two medals appear as very thin leaf metals with exogenous material on the back side, that does not show artistic details. The use of such thin strikings was unique to Alessandro Cesati (*ca.* 1505–1574 A.D.), a famous but not much-studied goldsmith, gem–cutter and medalist. He was nicknamed 'Il Greco' or 'Grechetto' ("The Greek") because he was born in Cyprus in the early 16th century. During the pontificate of Paul III Farnese (1534–1549 A.D.) Cesati became Master of the Roman Mint, and he probably used these specimens as struck samples but also as pieces to send to his patrons outside Rome, in order to make them acquainted with his uncommon artistic skills [17]. In particular, the medals here analysed were produced by Cesati for Pope Paul III (1534–1549 A.D.) and Pope Julius III (1550–1555 A.D.). There are no precise data on the composition of these exemplars given that they had never been analysed previously.

Since they were only assumed to be made of silver to date, we first investigate the nature of the metal used. We employ non-invasive and non-destructive analysis to clarify the peculiar use made by the artist of such thin uniface pieces and the technique used by Cesati to produce them. The elemental composition and the surface morphology are investigated with a Scanning Electron Microscope with an Energy Dispersive System (SEM-EDS). To complete the study, we use Fourier-Transform Infrared Spectroscopy (FTIR) to characterize the organic material on the back side of the samples.

Research aim

The aim of the present work is twofold: first, surface analysis will be undertaken to provide information on the metals and alloys used by Cesati for the creation of the foils, in order to unveil new data on the production of such objects and helping to reconstruct their history; second, these specimens have never been analysed before, so the data about their composition will enable their correct conservation. The analytical approach here adopted is non-destructive and non-invasive, since the samples are fragile and musealised. This research represents a peculiar case study thanks to the uniqueness of the objects, and it can open further discussions and scientific investigations on medals.

Experimental

Materials

The selected samples are shown in Fig. 1 and are inventoried as: 6262, 6269, and 6275. Medal 6262 was produced by Cesati for Pope Paul III (1534–1549 A.D.), whereas 6269 and 6275 were created for Pope Julius III (1550–1555 A.D.). As shown in Fig. 1a, 6269 actually indicates two objects, *i.e.* two metal foils, probably at some time connected (Fig. 1a). In fact, each foil has a decorated side (corresponding to the obverse and reverse of a medal) and a back side with no figuration and with traces of exogenous material. 6275 has just one metal foil with silver and polished appearance (Fig. 1b, the reverse and the back side of the reverse). Fig. 1c,d,e shows the medal 6262 and its details. 6262 has two foils glued to a central core, where residues of sticky material are visible, and is fragile since the metal foils are damaged and unstable, especially on the rounded edge, as depicted in Fig. 1d,e.

Methods

After a first observation of the surface *in situ* using a portable optical microscope, DINO Lite (digital microscope, AnMo Electronics Corporation), FTIR analysis was performed using handheld AGILENT 4100 ExoScan to characterize the exogenous material on the back sides of the obverse and reverse of 6269. Even if the interface of the instrument was in direct contact with the surface, the analysis was non-destructive and non-invasive. The spectra were acquired in external reflectance mode from 4000 to 650 cm^{-1}, and it did not require sample preparation. The spectral resolution was 4 cm^{-1}, 16 scans were acquired for the background and the sample under Happ-Genzel apodization [18–20]; the instrumental gain was set at 225. Gain is used to increase the intensity of weak detector signals and the background spectrum was acquired before the measurements. Three different points were analysed without any contact with the surface of the samples. The data were analysed with MicroLab Lite Software (version 1.1.), developed by Agilent Technologies. Scanning Electron Microscopy (SEM) imaging analysis, *i.e.*, secondary electrons (SE), backscattered electrons (BSE) and mixed signals and Energy Dispersive Spectroscopy (EDS) were performed at NEST laboratories (Scuola Normale Superiore, Pisa) using a TM4000 Plus II (Hitachi, Hitachi High-Tech Corporation, Tokyo, Japan). SEM-EDS data were acquired operating in high vacuum at accelerating voltage of 10 kV. The instru-

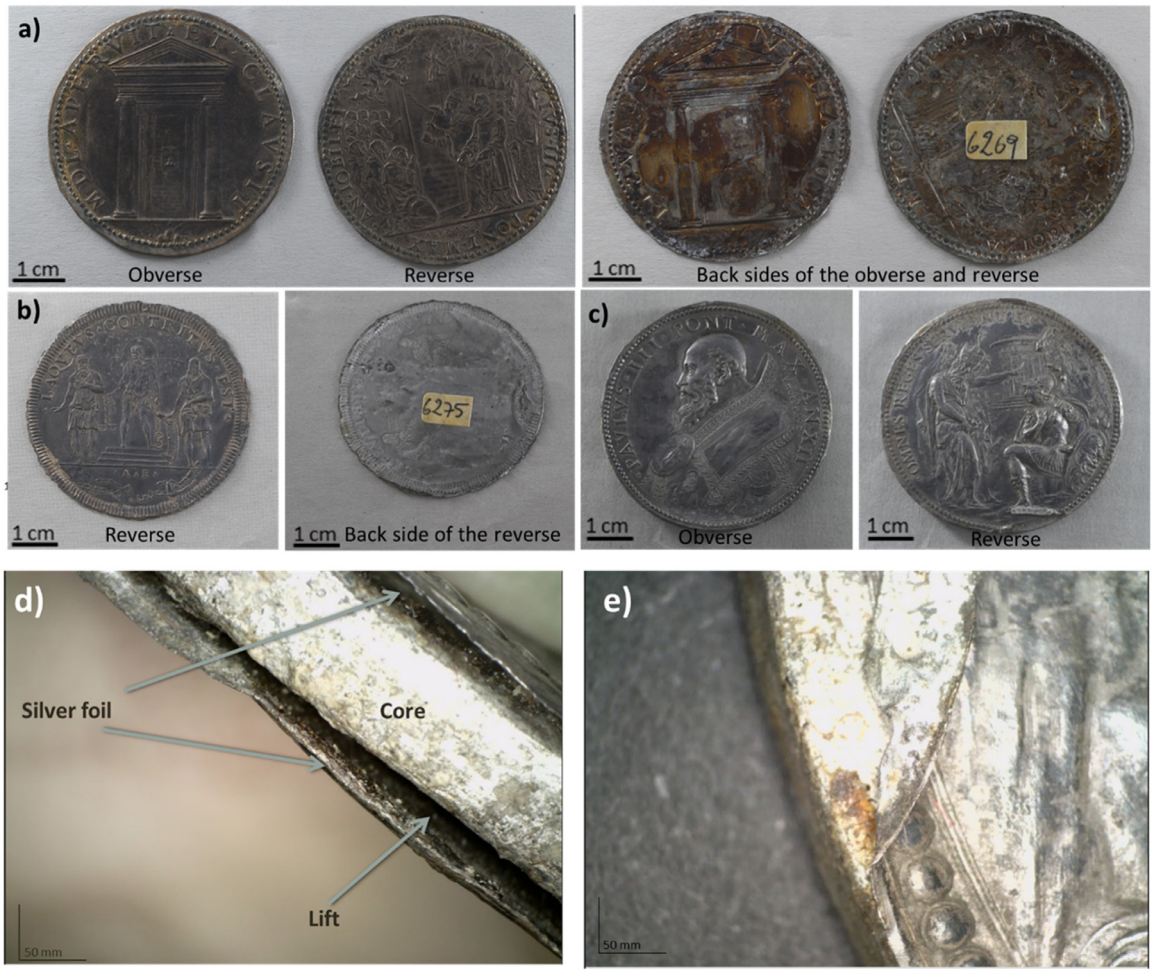

Fig. 1. (**a**) Obverse, reverse, and back sides of 6269; (**b**) reverse and its back side of 6275 and (**c**) obverse and reverse of 6262. (**d**) detail of 6262 and (**e**) the conservation issue of the foils glued on the substrate.

Table 1
EDS results of the elemental composition of the samples. The data are collected on three different spots on the metal surface, free of the exogenous brownish substance, to evaluate the chemical composition. Only one side (reverse) of 6262 was analysed due to the noticeable fragility of 6262.

Sample	Ag (wt%)	Au (wt%)	Cu (wt%)	Cl (wt%)	Pb (wt%)	Sn (wt%)	O (wt%)	C (wt%)	Other elements
6269	30.9	6.3	6.4	7.2	3.7	–	33.5	10.0	Ca, S, K, Si
Reverse	32.3	5.7	4.6	7.4	3.2	–	33.0	9.7	Ca, S, K, Si
	31.3	4.4	4.0	7.3	4.1	–	34.5	10.0	Ca, S, K, Si
Obverse	24.5	12.2	3.6	4.2	5.9	–	35.6	20.3	Ca, S, K, Si
	25.9	6.2	5.1	4.1	2.5	–	41.0	13.3	Ca, S, K, Si
	25.6	4.3	5.3	4.4	2.6	–	42.1	13.6	Ca, S, K, Si
6275	35.2	–	0.4	2.4	2.0	–	41.9	12.6	S, Ca, Si, K, P, Mg, Na, Al
Reverse	39.2	–	0.2	1.9	1.0	–	41.2	12.5	S, Si, Ca, Al, Na, P, Mg
	39.2	–	0.2	1.6	0.9		41.1	12.4	S, Si, Ca, K, Al, Na, P, Mg
Back side of the reverse	–	–	0.7	1.4	27.8	38.1	26.6	5.2	As
	0.6	–	6.0	1.9	19.0	17.1	42.2	12.7	S, P
	–	–	0.5	2.5	27.8	27.6	32.9	8.7	–
6262	47.5	–	0.3	1.6	–	–	35.9	10.3	S, Na, K, Ca, Si, Mg
Reverse	36.3	–	0.2	0.9	3.0	1.6	41.6	13.1	S, Na, Ca, Si, Mg
	48.0	–	0.3	1.4	–	–	36.2	11.1	S, Na, Ca, Si, Al

ment was equipped with High-Sensitivity 4-segment BSE detector, allowing the acquisition of the X-rays maps of the main elements on the surface. Only one side (reverse) of 6262 was analysed due to the noticeable fragility of 6262, and the analysis was carried out quickly without compromising 6262′s integrity in the high vacuum of the SEM chamber. EDS analyses are carried out on three different point of the surfaces and the obtained data are reported in Tables 1 and 2.

Results and discussion

SEM-EDS analysis

To investigate the surface morphology and metal composition, it was analysed by the means of SEM-EDS. EDS gives the semi-quantitative composition of the surface layers. Fig. 2a,b shows the mixed signals of the backscattered electrons (BSE) and sec-

Table 2
Composition of Sn- and Pb- rich areas indicated with numbers in Fig. 3c.

		Pb (wt%)	Sn (wt%)	O (wt%)	C (wt%)	Ag (wt%)	Cl (wt%)
Pb-rich area	1	55.3	16.1	23.0	5.4	–	–
	2	59.3	14.0	21.7	5.0	–	–
	3	64.3	24.2	11.5	–	–	–
Sn-rich area	4	8.4	59.9	27.6	4.1	–	–
	5	11.7	54.8	25.4	3.5	4.6	–
	6	12.1	57.2	26.2	3.7	–	0.8

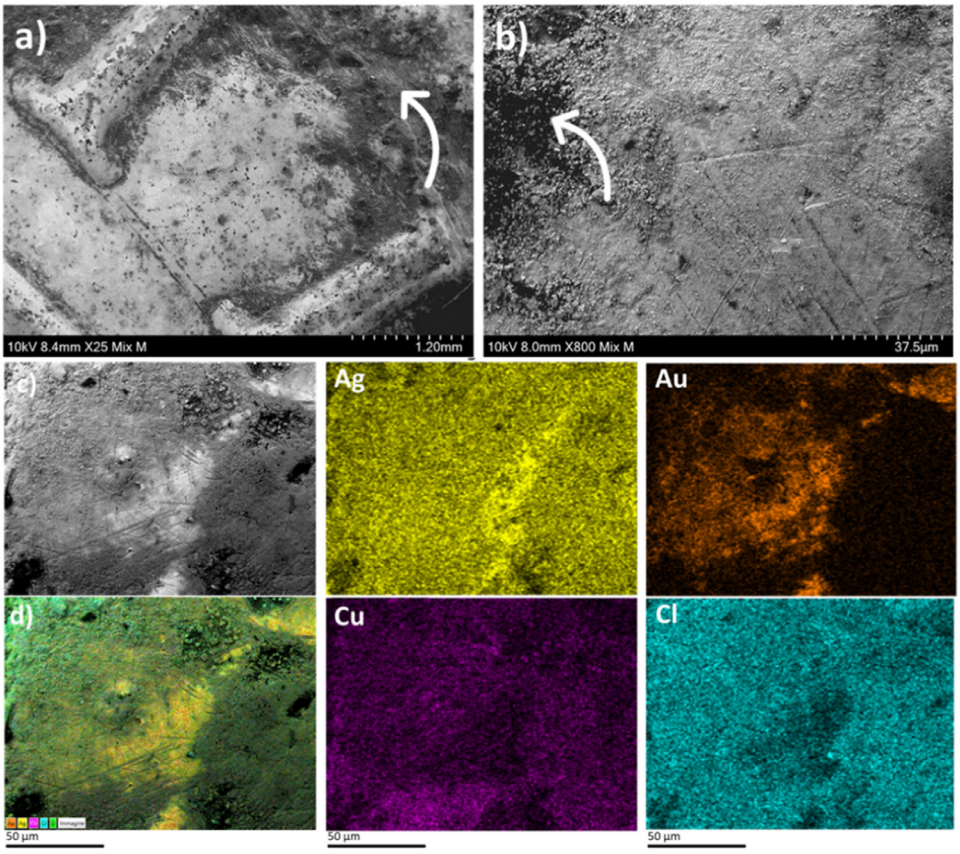

Fig. 2. (**a,b**) Mixed signal (SE and BSE) images of the surface morphology of 6269 surface; (**c**) BSE and SE of the analysed area and (**d**) images of the superimposed X-rays maps of the major elements detected.

ondary electrons (SE) on different areas of 6269. The surface shows deposits of dust and organic materials accumulated in the tiny craters, as indicated by the arrows. Nevertheless, the surface is smooth and well preserved, without corrosion problems, and the artistic details are visible and well-defined although some scratches (Fig. 2b), probably due to previous cleaning procedures. The smoothness suggests that the medals were produced by striking, due to the lack of two features of casted medals: i) air bubbles and ii) surface roughness [1,4,13]. The well-preserved and flat surface appearance is shared by all samples.

X-rays maps of Fig. 2 depict the elemental distribution of the major elements found on the surface of 6269. The analysis was also carried out in other two areas, and the corresponding maps are given in Figures 1S and 2S of *Supplementary Materials*. The back side of 6269, showing a brownish organic material, is analysed by FTIR (*vide infra*). Table 1 reports the semi-quantitative analysis performed on this area, revealing the particular composition of the foil. Here, Au is between 4.3 and 6.3 wt% (reverse) and between 4.4 and 12.2 wt% (obverse); Ag is between 30.9 and 32.3 wt% in the reverse and between 24.5 and 25.9 wt% in the obverse. The range of Cu goes from 4.6 to 6.4 wt% in the reverse and from 3.6 to 5.3 wt% in the obverse. Au, Ag and Cu constitute the alloy of the obverse and the reverse of 6269. Pb is probably also part of the used alloy, even if it is present in lower percentages (from 2.5 up to 5.9 wt% considering reverse and obverse). Cl is a contaminant element, present on the surface in the highest percentages. Ca, Si, K, Si are also external elements, detected in lower quantities, whose presence is due to the handling of the medals. It is possible to assume that Ag and Au were used as polish, giving a precious appearance to the samples. In early modern times, artists used plating methods to apply precious metals to cheaper materials. The most challenging aspect in this process was to obtain thin layers of Ag or Au which covered the entire surface, guaranteeing the fine aspect of the medal [7,21]. However, given Cesati's skill as a goldsmith, he masterfully produced such plated foils. The plating process allowed him to save on precious metals because these medals were likely used as prototypes to send from Rome to friends or new patrons to prove his artistic skills.

The use of the plating method can be verified with the analysis of the back side of 6275: in fact, the plating method regards only the decorated surfaces – the obverse and the reverse – whereas the back sides are supposedly made of a less precious alloy. BSE

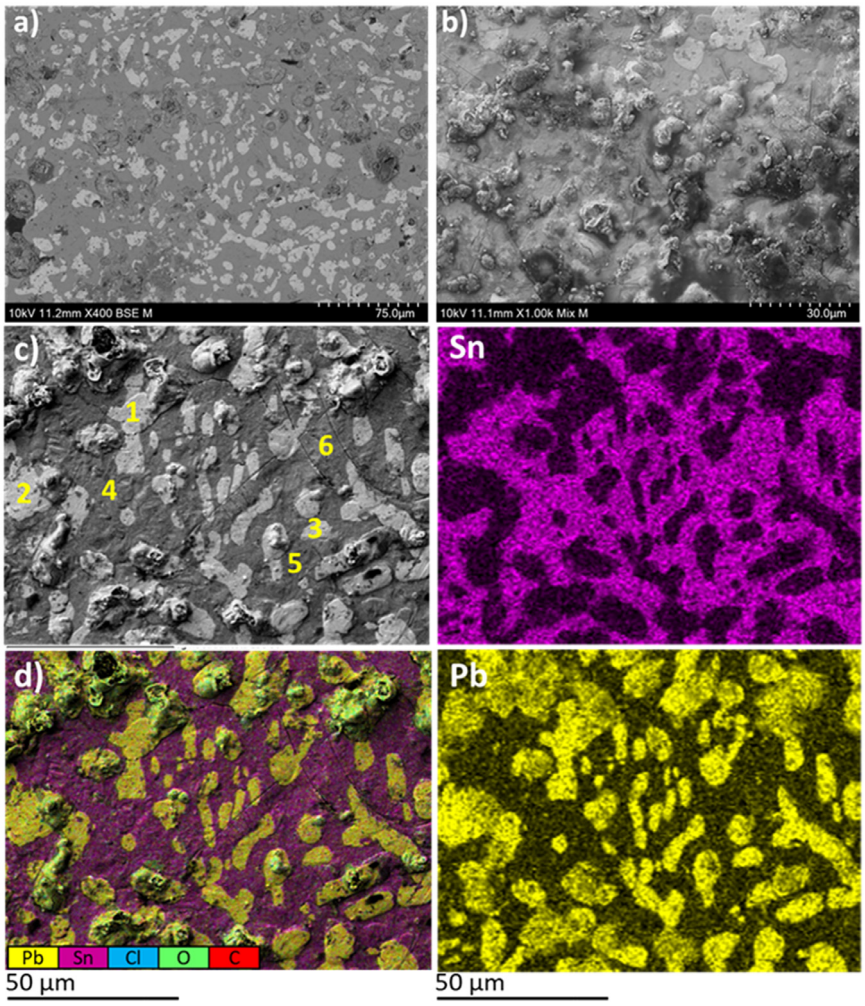

Fig. 3. (**a,b**) BSE and mixed signal of the back side of 6275; (**c**) BSE and (**d**) images of the superimposed X-rays maps of the major elements detected. Numbers in (**c**) indicate the analysed areas and for the elemental composition of Table 2.

and the mixed signal are shown in Fig. 3a-d. The analysis reveals the original alloy of the medals: islands of Pb immersed in a matrix of Sn, clearly distinguishable in the X-rays maps of Fig. 3d. The microstructure visible in Fig. 3 is typical of such alloys, where the portioning of Sn and Pb is due to the low solubility of Pb into Sn, and Pb remains in a liquid state up to the eutectic temperature (183 °C in Sn-Pb alloy) [22,23]. The typical microstructure of a Pb-Sn alloy is due to the substantial non-solubility of Pb in Sn in the solid state, forming a dispersion of islands throughout a matrix of Sn. The number and the distribution of Pb islands depends on several factors: Pb content, casting temperature, and cooling rate. If the cooling rate is slow, Pb can form aggregates of relevant dimensions, as it is rejected by the freezing edge [24–27]. The distribution of Pb island appears quite random, suggesting that there is no preferential trend due to the mechanical processing of the foil; moreover, the dimension of the lead aggregates supports the idea that the alloy has a slow cooling rate, solidifying gradually and thus allowing the clustering of Pb. The content of Sn in Sn-rich areas is calculated: it is up to 59.9 wt%, and in the islands, Pb reaches 64.3 wt% (Table 2). Ag (4.6 wt%) and Cl (0.8 wt%) are also detected in the Sn-rich areas. The surface morphology of the back side supports the striking and plating as the most probable method used to produce such exemplars. The presence of Ag (0.6 wt% in the area of Fig. 3d, Table 1, and 4.6 wt% in Sn-rich area, Table 2) can be considered as either residue of the plating or imperfect lead processing, starting from its extraction from the *argentiferous Galena* (PbS) [10,28,29]. The extensive use of Pb facilitates both the manipulation of a metallic liquid alloy more easily and the engraving of the final product [24,30,31]. Cesati knew that the variations of the elemental composition affect its mechanical properties: the machinability is improved by adding Pb in high percentages (up to 2%), making the production easier. On the other hand, lead reduces the hardness of the alloy [31]. On the decorated side (the reverse), plating hides this microstructure, as well as the Sn and Pb elements: the composition of the reverse, in fact, is characterised mainly by Ag (35.2 - 39.2 wt%) and other elements (S, Ca, Si, K, P, Mg, Na, Al), being similar to the sample 6269. As depicted in Figure 3S of *Supplementary Materials*, the reverse is silvered, whereas the back side is made of Sn-Pb alloy.

The same analyses were performed on the surface of sample 6262, which appears fragile with two foils pasted onto a central body. These foils are raised and damaged in several areas (Fig. 1d,e). To reduce potential stress for the object only one side is analysed. Surface analysis returns results similar to the other samples: the main element is Ag (from 36.3 wt% up to 48.0 wt%). Pb is not present, or it reaches just 0.3 wt%. Copper too has a low percentage (from 0.2 to 0.3 wt%). Cl is detected ranging between 0.9 to 1.6 wt%. SE, BSE and X-rays maps given in *Supplementary Materials* (Fig. 4S) highlight that the surface is quite uniform in composition, confirming the possibility that plating was used to cover

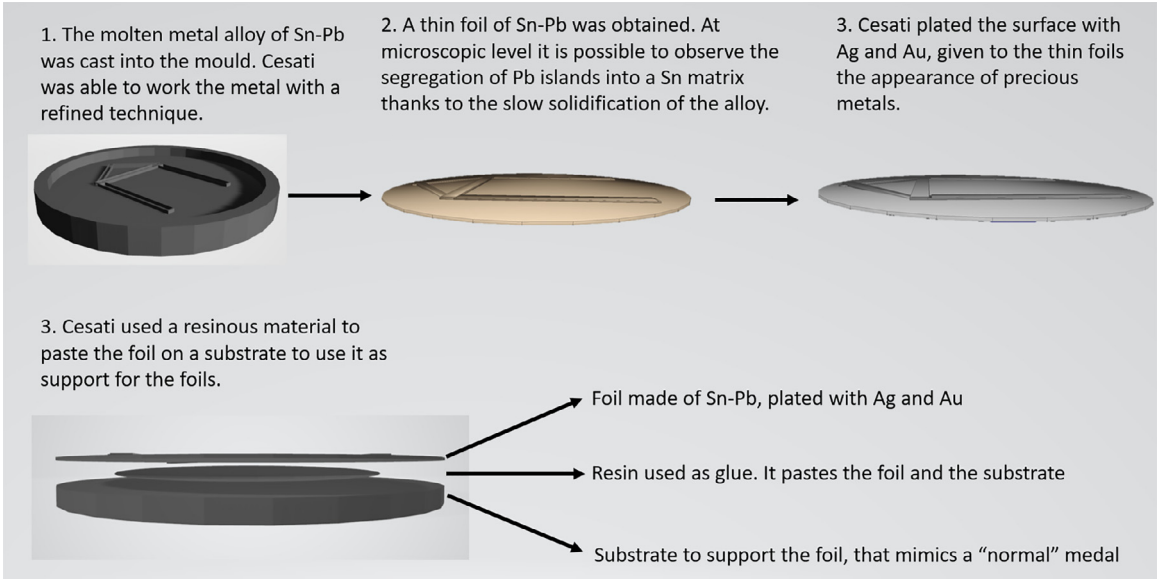

Fig. 4. Schematic representation of the manufacturing of the thin uniface metallic strikings by Alessandro Cesati according to the data collected.

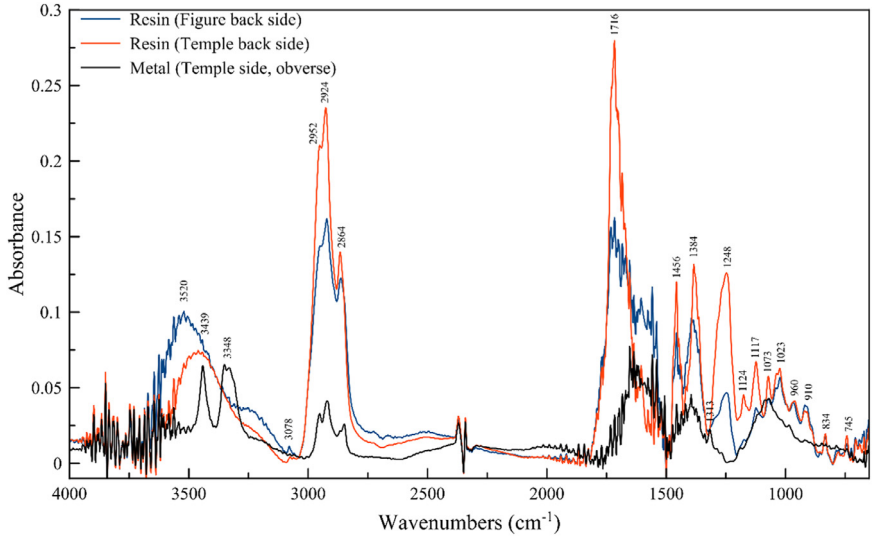

Fig. 5. FTIR spectra of medal 6269 of the organic material analysed on the back side of the two foils (blue and red), and the spectra obtained on the metal surface, free of the exogenous brownish substance (black). The spectra were acquired in external reflectance mode from 4000 to 650 cm^{-1}. The spectral resolution was 4 cm^{-1}, 16 scans were acquired for the background and the sample; the instrumental gain is set at 225.

the surface. Sample 6262 gives an important hint about the overall structures of the uniface strikings. The process of production is schematically depicted in Fig. 4: the artist cast an alloy of Pb-Sn into the mold, obtaining very thin foils. To give them a precious appearance, these foils were plated with Ag, Au and Cu. The metal leaves were then glued on a substrate which came to us only in the case of 6262.

FTIR analysis

FTIR analysis is commonly used in Cultural Heritage field to perform *in-situ,* non-destructive and non-invasive analysis. As reported in literature, such materials are difficult to be analysed, especially for the surface roughness, which can influence the IR response [32,33]. In our case, the organic material is amply spread on the back side of the obverse and reverse of medal 6269. This suggests the use of a resin to paste the two laminas onto the core metal, obtaining an object similar to 6262. Natural resins, which were extensively used in the past, are heterogeneous and complex mixtures of organic compounds, with diterpenoids and triterpenoids making up the soluble and non-volatile part [34,35]. Comparing the spectra obtained by the analysis of the organic material (Fig. 5) with the literature [35–42], it is possible to identify the characteristic compounds of ancient resins, especially mastic. The region between 3600 and 3200 cm^{-1} indicates the presence of free –OH stretching [35,39]. The spectrum of the metal in Fig. 5 and 5S shows two bands in the -OH stretching region at 3439 and 3348 cm^{-1}. These peaks can be attributable to the presence of copper hydroxychlorides, whose signals fall in this region [43–46]. The strong bands present on 2952, 2924 and 2864 cm^{-1} are the symmetric and asymmetric stretching of CH_2 and CH_3 groups [35]. The peak at 1716 cm^{-1} is the carbonyl stretching band, found in the reference spectra of mastic [35,36,39]. Other characteristic signs of natural resins are the bands at 1456 cm^{-1} (the bending of CH_2 and the asymmetric bending of CH_3); 1384 cm^{-1} (the symmetric bending of CH_3 groups) and 1248 cm^{-1} (C–O stretching of ester groups)

[35,38,47]. According to literature, resins can be distinguished from carbohydrates, waxes, and oils by the presence of two bands: the first between 1750 and 1700 cm^{-1} and the second between 1380 and 1390 cm^{-1}, both visible in the spectra of Fig. 5 [48]. The fingerprint region (starting from 1200 cm^{-1}) has several peaks, not allowing the precise identification of the compounds but supporting the hypothesis of a natural resin applied on the foils [48].

The same signals are found in the metal spectra of 6262 and 6275 (Fig. 5S of *Supplementary Materials*), where the O–H region is noisy or very broadened ($\sim$ 3595 cm^{-1}) and the strong bands present at 2952, 2924 and 2864 cm^{-1} are still present. The prominent peak at 1716 cm^{-1} was not detected, and this is reasonable because the analysis was carried out on the metal, which can be responsible for the noisy signal of the entire spectra.

It is common knowledge that FTIR allows to determine the functional groups of the samples, even if the identification of heterogeneous materials can be difficult, especially in the case of materials such as resins. There are several factors influencing the response: the crystallinity of the analysed compounds and the surface roughness are the most common factors leading to the distortions of shape bands [49]. This contributes to the accurate identification of the components of a mixed material. In this case, it is possible to classify the functional group that determines belonging to a certain class of compounds. However, it is impossible the univocally identify the spectrum, also considering the possible contributions of undocumented restorations and the handling of the medals over the centuries. The difficulty in unequivocal identification of surface compounds also lies in the presence of several contributions, such as that of silicates, identifiable with the peak at 1081 cm^{-1} [50–52] in the spectrum shown in Figure 5S.

Based on the data acquired, and its comparison with literature results [35,53,54] it can be assumed that the organic material found on the metal surface could be a vegetal resin, especially mastic, used as glue by many artists in the past [55–58]. Mastic is a hard, brittle substance with orange, yellow or brownish colours. The resins are amorphous, insoluble in water and soluble in organic solvents, and are mainly characterized by terpenes and their derivatives. The most common resins are bicyclic and monocyclic terpenes and, in smaller amounts, by tricyclic ones. Almost all resins also contain a high proportion of resin acids: these are closely related to the terpenes when derived from partial terpene oxidation. The large number of types, the complexity, and the variety of their composition, as well as their frequent changes over time due to oxidation or polymerization process, makes the precise identification of resins difficult.

Conclusions

In this work the elemental composition and the surface morphology of specimens coming from the Bargello Museum were investigated by the means of SEM-EDS. Based on the discussed results, we conclude that Cesati produced the foils with an inexpensive alloy (Sn-Pb) plated with Ag and Au.

The foils were mechanically worked with a soft hammering because no preferential orientation of Pb islands was observed during the SEM analysis. Moreover, the dimensions of the Pb aggregates indicate that the cooling rate of the alloy was slow, permitting the separation of lead from the tin. FTIR analysis helped in the identification of resinous material on 6269. This was also visible, but not analysable, on 6262. The resin was used to paste the foils on a poor metallic support. Organic glues are commonly employed in artistic techniques to adhere a thin metal on another layer (*i.e.*, in the gilding method). This research was carried out on unique artistic pieces coming from a Public museum, allowing us to know the composition of the examined exemplars for the first time. The scientific data here obtained are an essential contribution to historical research and help to answering pivotal questions regarding Cesati and his production abilities. The obtained data enriches the knowledge about the Renaissance medals and suggests a path for new research topics.

Author contributions

F.D. wrote the manuscript, acquired, and interpreted the SEM-EDS and FTIR data with the contribution of other authors. G.D. wrote the historical context, under the supervision of L.S. P.D. supervised the research work on medals in the Bargello Museum. L.S. coordinated the MeB project and supervised the historical context. F.B. and P.P. supervised and coordinated the scientific analysis.

Funding

The project has been co-financed by POR FSE TOSCANA 2014–2020 within the 'GiovaniSì' project (www.giovanisi.it), promoted by Regione Toscana. Funding by Laboratorio di Documentazione Storico-Artistica (DocStAr), Scuola Normale Superiore are thanked for the support during the revision of the manuscript.

Acknowledgements

This article has been elaborated within the MeB Project ('Conoscere e conservare i piccoli metalli del Bargello: nuove indagini storico-artistiche e scientifiche su medaglie e placchette d'età moderna', 2020–2022). We thank the funding of the European Union, the Italian Republic, the Tuscany Region and Scuola Normale Superiore. The acknowledgments go to Dr. Giandonato Tartarelli (Scuola Normale Superiore) for his support on the photographic campaign on the Bargello's collection. We thank Dr. Aldo Moscardini (NEST laboratories, Scuola Normale Superiore) for the fruitful discussion about FTIR and Dr. Matthys van Huyssteen, who revised the English language of the manuscript. The medals' photos copyright belongs to ©MiC - Musei del Bargello, Firenze.

Supplementary materials

Supplementary material associated with this article can be found, in the online version, at doi:10.1016/j.culher.2023.05.034.

References

[1] L.A. Glinsman, Renaissance portrait medals by Matteo de' Pasti : a study of their casting materials, in: Studies on History of Art, Monograph, National Gallery of Art, 1997, pp. 92–107.
[2] L. Simonato, Impronta Di Sua Santità. Urbano VIII e Le Medaglie, 1st ed., Scuola Normale Superiore, Pisa, 2008.
[3] S.K. Scher, in: Perspectives on the Renaissance Medals, Garland Publishing, Inc, 2000, pp. 15–23.
[4] P. Tuttle, Sided medals an investigation of the Renaissance casting techniques of double-sided medals, in: Studies in History of Art, National Gallery of Art, 1987, pp. 205–212.
[5] N. Orazi, The study of artistic bronzes by infrared thermography: a review, J. Cult. Herit. 42 (2020) 280–289, doi:10.1016/j.culher.2019.08.005.
[6] M.R. Villani, Il modo di far medaglie per stampare in acciaio, e così il modo dello stampar monete: appunti di tecnica sugli scritti di Benvenuto Cellini, in: Le Arti a Dialogo, 1st ed., Scuola Normale Superiore, Pisa, 2015, pp. 1–326.
[7] G.M. Ingo, S. Balbi, T. de Caro, I. Fragalà, C. Riccucci, G. Bultrini, Microchemical investigation of Greek and Roman silver and gold plated coins: coating techniques and corrosion mechanisms, Appl. Phys. A Mater. Sci. Process. 83 (2006) 623–629.
[8] R. Linke, M. Schreiner, G. Demortier, M. Alram, Determination of the provenance of medieval silver coins: potential and limitations of x-ray analysis using photons, electrons or protons, X-Ray Spectrom. 32 (2003) 373–380, doi:10.1002/xrs.654.
[9] L. Fabrizi, F. di Turo, L. Medeghini, M. di Fazio, F. Catalli, C. de Vito, The application of non-destructive techniques for the study of corrosion patinas of ten Roman silver coins: the case of the medieval Grosso Romanino, Microchem. J. 145 (2019) 419–427, doi:10.1016/j.microc.2018.10.056.
[10] F. Di Turo, Limits and perspectives of archaeometric analysis of archaeological metals: a focus on the electrochemistry for studying ancient bronze coins, J. Cult. Herit. (2020), doi:10.1007/978-3-319-12616-6.

[11] M.T. Doménech-Carbó, C. Álvarez-Romero, A. Doménech-Carbó, L. Osete-Cortina, M.L. Martínez-Bazán, Microchemical surface analysis of historic copper-based coins by the combined use of FIB-FESEM-EDX, OM, FTIR spectroscopy and solid-state electrochemical techniques, Microchem. J. 148 (2019) 573–581, doi:10.1016/j.microc.2019.05.039.
[12] E. Farrell, Non-destructive instrumental analysis of medals, Stud. Hist. Art 21 (1987) 35–43.
[13] D. Barbour, L.D. Glinsman, An investigation of renaissance casting practices as a means for identifying forgeries, Stud. Hist. Art 41 (1993) 14–29.
[14] A. Beale, Surface characteristics of renaissance medals and their interpretation, Stud. Hist. Art 21 (1987) 386–408.
[15] G. Wharton, Technical examination of Renaissance medals the use of Laue back reflection X-ray diffraction to identify electroformed reproductions, J. Am. Inst. Conserv. 23 (1984) 88–100, doi:10.1179/019713684806028232.
[16] L.A. Glinsman, L.C. Hayek, Multivarlite analysis of renaissance portrait medals: an expanded nomenclature for defining alloy composition, Archaeometry 35 (1993) 49–67, doi:10.1111/j.1475-4754.1993.tb01023.x.
[17] G. Daniele, Toward a 1550 'double Jubilee' medal by Alessandro Cesati, Unpublished Results. (2023).
[18] G. Jalsovszky, Resolution errors in FTIR absorbance measurements, J. Mol. Struct. 114 (1984) 127–132.
[19] R.S. Bretzlaff, T.B. Bahder, Apodization effects in Fourier transform infrared difference spectra, Revue de Physique Appliquée 21 (1986), doi:10.1051/rphysap:019860021012083300.
[20] S. Egbert, C. Carpenter, Comparison of FTIR apodization functions using modeled and measured spectral data, J. Appl. Eng. Math. 4 (2017) 1–4.
[21] G.M. Ingo, M. Albini, A.D. Bustamante, S. del P. Zambrano Alva, A. Fernandez, C. Giuliani, E. Messina, M. Pascucci, C. Riccucci, P. Staccioli, G. di Carlo, L. Tortora, Microchemical investigation of long-term buried gilded and silvered artifacts from ancient Peru, Front. Mater. 7 (2020), doi:10.3389/fmats.2020.00230.
[22] F. Zu, X. Fen Li, L. Liu, R. Shen, Z. Chen, Abnormal solidification of Pb-Sn alloy induced by liquid structure transition, Kokove Materialy 43 (2005) 432–439.
[23] F. di Turo, F. Coletti, C. de Vito, Investigations on alloy-burial environment interaction of archaeological bronze coins, Microchem. J. 157 (2020) 104882, doi:10.1016/j.microc.2020.104882.
[24] M. Quaranta, E. Catelli, S. Prati, G. Sciutto, R. Mazzeo, Chinese archaeological artefacts: microstructure and corrosion behaviour of high-leaded bronzes, J. Cult. Herit. 15 (2014) 283–291, doi:10.1016/j.culher.2013.07.007.
[25] P.T. Craddock, The composition of the copper alloys used by the Greek, etruscan and Roman civilisations. 2. The Archaic, Classical and Hellenistic Greeks, J. Archaeol. Sci. 4 (1977) 103–123, doi:10.1016/0305-4403(77)90058-9.
[26] S. la Niece, P. Craddok, Metal plating and patination, Metal Plating and Patination. (1993) 135–147. https://doi.org/10.1016/B978-0-7506-1611-9.50015-7.
[27] G.M. Ingo, T. de Caro, C. Riccucci, S. Khosroff, Uncommon corrosion phenomena of archaeological bronze alloys, Appl. Phys. A Mater. Sci. Process. 83 (2006) 581–588, doi:10.1007/s00339-006-3534-z.
[28] T. de Caro, The ancient metallurgy in Sardinia (Italy) through a study of pyrometallurgical materials found in the archaeological sites of Tharros and Montevecchio (West Coast of Sardinia), J. Cult. Herit. 28 (2017) 65–74, doi:10.1016/j.culher.2017.05.016.
[29] C. Gasparrini, G.R. Lowell, Silver bearing inclusions in argentiferous galena from the silvermine district in southeastern Missouri, Can. Mineral. 23 (1985) 99–102.
[30] M. Griesser, W. Kockelmann, K. Hradil, R. Traum, New insights into the manufacturing technique and corrosion of high leaded antique bronze coins, Microchem. J. 126 (2016) 181–193, doi:10.1016/j.microc.2015.12.002.
[31] F. di Turo, N. Montoya, J. Piquero-Cilla, C. de Vito, F. Coletti, G. Favero, M.T. Doménech-Carbó, A. Doménech-Carbó, Dating archaeological strata in the magna mater temple using solid-state voltammetric analysis of leaded bronze coins, Electroanalysis 30 (2018) 361–370.
[32] C. Miliani, F. Rosi, B.G. Brunetti, A. Sgamellotti, In situ noninvasive study of artworks: the MOLAB multitechnique approach, Acc. Chem. Res. 43 (2010) 728–738, doi:10.1021/ar100010t.
[33] I. Arrizabalaga, O. Gómez-Laserna, J. Aramendia, G. Arana, J.M. Madariaga, Applicability of a diffuse reflectance infrared Fourier transform handheld spectrometer to perform *in situ* analyses on Cultural Heritage materials, Spectrochim. Acta A Mol. Biomol. Spectrosc. 129 (2014) 259–267, doi:10.1016/j.saa.2014.03.096.
[34] K. van den Berg, J. van der Horst, J.J. Boon, O.O. Sudmeijer, Cis-1,4-poly-B-myrcene: the structure of polymeric fraction of mastic resin (Pistacia Lentiscus) elucidated, Tetrahedron Lett. 39 (1998) 2645–2648 0040-4039/98/$19.00.
[35] S. Bruni, V. Guglielmi, Identification of archaeological triterpenic resins by the non-separative techniques FTIR and 13C NMR: the case of Pistacia resin (mastic) in comparison with frankincense, Spectrochim. Acta A Mol. Biomol. Spectrosc. 121 (2014) 613–622, doi:10.1016/j.saa.2013.10.098.
[36] S. Zareva, I. Kuleff, The application of the derivative IR-spectroscopy and HPLC-ESI-MS/MS in the analysis of archaeology resin, Spectrochim. Acta A Mol. Biomol. Spectrosc. 76 (2010) 283–286, doi:10.1016/j.saa.2010.03.021.
[37] P.E. McGovern, G.R. Hall, Charting a future course for organic residue analysis in archaeology, J. Archaeol. Method Theory 23 (2016) 592–622, doi:10.1007/s10816-015-9253-z.
[38] E. Casanova, C. Pelé-Meziani, É. Guilminot, J.Y. Mevellec, C. Riquier-Bouclet, A. Vinçotte, G. Lemoine, The use of vibrational spectroscopy techniques as a tool for the discrimination and identification of the natural and synthetic organic compounds used in conservation, Anal. Methods 8 (2016) 8514–8527, doi:10.1039/c6ay02645a.
[39] G. Abdel-Maksoud, H. El-Shemy, M. Abdel-Hamied, Investigation methods for evaluating the preservative organic mixtures applied on a Late Period mummy, Archaeol. Anthropol. Sci. 11 (2019) 1843–1850, doi:10.1007/s12520-018-0633-7.
[40] L. Bonizzoni, S. Bruni, M. Gargano, V. Guglielmi, C. Zaffino, A. Pezzotta, A. Pilato, T. Auricchio, L. Delvaux, N. Ludwig, Use of integrated non-invasive analyses for pigment characterization and indirect dating of old restorations on one Egyptian coffin of the XXI dynasty, Microchem. J. 138 (2018) 122–131, doi:10.1016/j.microc.2018.01.002.
[41] Y.H. Yu, Y.P. Feng, W. Liu, T. Yuan, Diverse triterpenoids from mastic produced by Pistacia lentiscus and their anti-inflammatory activities, Chem. Biodivers. 19 (2022), doi:10.1002/cbdv.202101012.
[42] M. Ménager, C. Azémard, C. Vieillescazes, Study of Egyptian mummification balms by FT-IR spectroscopy and GC–MS, Microchem. J. 114 (2014) 32–41, doi:10.1016/j.microc.2013.11.018.
[43] J. Buse, V. Otero, M.J. Melo, New insights into synthetic copper greens: the search for specific signatures by raman and infrared spectroscopy for their characterization in medieval artworks, Heritage 2 (2019) 1614–1629, doi:10.3390/heritage2020099.
[44] N. Salvadó, S. Butí, M. Cotte, G. Cinque, T. Pradell, Shades of green in 15th century paintings: combined microanalysis of the materials using synchrotron radiation XRD, FTIR and XRF, Appl. Phys. A Mater. Sci. Process. 111 (2013) 47–57, doi:10.1007/S00339-012-7483-4/FIGURES/6.
[45] P. Knipe, K. Eremin, M. Walton, A. Babini, G. Rayner, Materials and techniques of Islamic manuscripts, Herit. Sci. 6 (2018) 1–40, doi:10.1186/S40494-018-0217-Y/FIGURES/28.
[46] L. Monico, F. Rosi, C. Miliani, A. Daveri, B.G. Brunetti, Non-invasive identification of metal-oxalate complexes on polychrome artwork surfaces by reflection mid-infrared spectroscopy, Spectrochim. Acta A Mol. Biomol. Spectrosc. 116 (2013) 270–280, doi:10.1016/J.SAA.2013.06.084.
[47] J.S. Gaffney, N.A. Marley, D.E. Jones, Fourier Transform Infrared (FTIR) Spectroscopy, in: E. N. Kaufmann (Ed.), 1st ed., John Wiley & Sons, Inc., 2012: pp. 1104–1134.
[48] P. Martín-Ramos, I.A. Fernández-Coppel, N.M. Ruíz-Potosme, J. Martín-Gil, Potential of ATR-FTIR spectroscopy for the classification of natural resins, Biol., Eng., Med. Sci. Rep. 4 (2018) 03–06, doi:10.5530/bems.4.1.2.
[49] F. Izzo, C. Germinario, C. Grifa, A. Langella, M. Mercurio, External reflectance FTIR dataset (4000–400 cm−1) for the identification of relevant mineralogical phases forming Cultural Heritage materials, Infrared Phys. Technol. 106 (2020) 103266, doi:10.1016/j.infrared.2020.103266.
[50] S. Bruni, F. Cariati, F. Casadio, L. Toniolo, Spectrochemical characterization by micro-FTIR spectroscopy of blue pigments in different polychrome works of art, Vib. Spectrosc. 2′ (1999) 15–25.
[51] L. Medeghini, S. Mignardi, C. De Vito, A.M. Conte, Evaluation of a FTIR data pretreatment method for Principal Component Analysis applied to archaeological ceramics, Microchem. J. 125 (2016) 224–229, doi:10.1016/j.microc.2015.11.033.
[52] L. Damjanović, V. Bikić, K. Šarić, S. Erić, I. Holclajtner-Antunović, Characterization of the early Byzantine pottery from Caričin Grad (South Serbia) in terms of composition and firing temperature, J. Archaeol. Sci. 46 (2014) 156–172, doi:10.1016/j.jas.2014.02.031.
[53] S. Prati, G. Sciutto, R. Mazzeo, C. Torri, D. Fabbri, Application of ATR-far-infrared spectroscopy to the analysis of natural resins, Anal. Bioanal. Chem. 399 (2011) 3081–3091, doi:10.1007/S00216-010-4388-Y/TABLES/3.
[54] C. Azémard, C. Vieillescazes, M. Ménager, Effect of photodegradation on the identification of natural varnishes by FT-IR spectroscopy, Microchem. J. 112 (2014) 137–149, doi:10.1016/J.MICROC.2013.09.020.
[55] L. Ghezzi, C. Duce, L. Bernazzani, E. Bramanti, M.P. Colombini, M.R. Tiné, I. Bonaduce, Interactions between inorganic pigments and rabbit skin glue in reference paint reconstructions, J. Therm. Anal. Calorim. 122 (2015) 315–322, doi:10.1007/s10973-015-4759-x.
[56] A. Bridarolli, A.A. Freeman, N. Fujisawa, M. Łukomski, Mechanical properties of mammalian and fish glues over range of temperature and humidity, J. Cult. Herit. 53 (2022) 226–235, doi:10.1016/j.culher.2021.12.005.
[57] J. Li, B. Zhang, Study of identification results of proteinous binding agents in Chinese painted cultural relics, J. Cult. Herit. 43 (2020) 73–79, doi:10.1016/j.culher.2019.12.015.
[58] P. Dietemann, C. Higgitt, M. Kälin, M.J. Edelmann, R. Knochenmuss, R. Zenobi, Aging and yellowing of triterpenoid resin varnishes - influence of aging conditions and resin composition, J. Cult. Herit. 10 (2009) 30–40, doi:10.1016/j.culher.2008.04.007.